EXPERIMENTAL INVESTIGATION OF THIN-FILM EVAPORATION IN AN OPEN-LOOP COLUMNATED MICRO-EVAPORATOR

Navdeep S. Dhillon*, **Christopher Hogue, Jim C. Cheng, Albert P. Pisano**
Department of Mechanical Engineering, University of California, Berkeley, United States
*Presenting Author: ndhillon@me.berkeley.edu, dr.ndhillon@gmail.com

Abstract: An open-loop columnated micro-evaporator has been designed, fabricated, and tested to characterize the process of thin-film evaporation in a microfluidic electronics cooling device. The micro-evaporator was fabricated on a silicon wafer using MEMS microfabrication techniques, and assembled with a ceramic heater and external liquid supply. An infrared thermal imaging system was used to measure the in-plane apparent thermal conductivity of the vapor chamber, which correlates to the rate of evaporation in the device. Unsteady thin-film evaporation in the vapor chamber was confirmed, with measured in-plane apparent thermal conductivities as large as 9500 W/mK.

Keywords: thin-film evaporation, microscale boiling, wick, vapor chamber, infrared imaging, micro loop heat pipe

INTRODUCTION

With the increasing density of transistors on a chip, the power dissipated per unit area of electronic substrates has become higher than ever [1]. With conventional thermal management solutions no longer feasible, new technologies are being investigated in order to avoid the thermal precipice facing the electronics industry. Loop heat pipes (LHPs) belong to a class of passive, phase change, high-heat-flux thermal management systems that are being actively pursued in this regard. Since conventional LHPs were bulky and fabricated out of non-planar metal tubing, miniaturized versions are now being developed for use in small electronic packages. While one approach has been to simply miniaturize the bigger versions [2, 3], other researchers have suggested fabricating these devices on planar silicon substrates [4–7].

In the LHP, latent heat of evaporation of the working fluid is used to transfer heat from an evaporator section to a condenser section. The fluid flow loop is driven by surface tension related capillary forces developed across the liquid-vapor meniscus in the wicking structure. Device performance depends on a number of parameters, one of which is the rate of evaporation in the wicking structure. We are working to develop a planar micro-columnated loop heat pipe ($\mu CLHP$), where a vertically-wicking dual-scale coherent porous silicon (CPS) wicking structure is employed to effect capillary wicking and phase change in the evaporator section [8, 9]. In this paper, we have implemented an experimental setup to characterize the process of thin-film evaporation in an open-loop columnated micro-evaporator. The open-loop micro-evaporator substitutes the capillary pumping mechanism of the CPS wick with an external syringe pump; This allows for a characterization of the phase change and heat transfer characteristics of the dual-scale micro-columnated wick, independent of the actual capillary pumping mechanism, which is attributed to the CPS pores of the micro-columnated wicking structure [10].

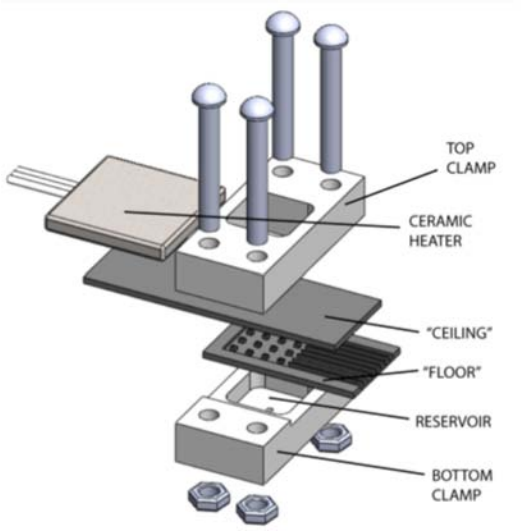

Fig. 1: Design and assembly of the open-loop columnated micro-evaporator for studying thin-film evaporation in a micro-columnated wicking structure.

MATERIALS AND METHODS

Open-Loop Columnated Micro-Evaporator

Fig. 1 shows the individual design and overall assembly of the open-loop micro-evaporator. It consists of two etched silicon wafers, which are clamped together to form a two-layer sandwich enclosing the columnated vapor chamber. Each layer is fabricated on a six inch $625\ \mu m$-thick silicon wafer, which is diced to the individual device dimensions. The bottom layer is approximately $24\ mm$ long and $14\ \mu m$ wide, and consists of a $10\ mm \times 10\ mm$ etched-out vapor chamber containing an orthogonal array of regularly-spaced hollow columns. Connecting the vapor chamber to the ambient are eight parallel vapor channels, each of which is $10\ mm$ long, $1\ mm$ wide, and approximately $200\ \mu m$ deep.

The top layer, or ceiling, consists of a $10\ mm \times 10\ mm$ region of uniformly patterned microtextures on

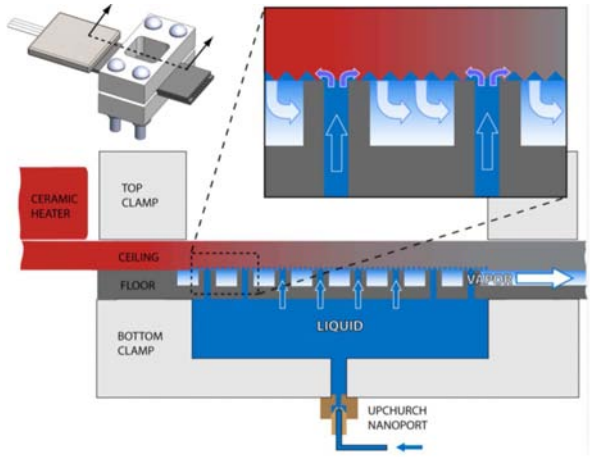

Fig. 2: Mechanism of operation of the micro-evaporator: Liquid supplied by an external syringe pump feeds the fluid reservoir; The columns convey the liquid to the ceiling, where it evaporates and exits through the vapor channels.

an otherwise plain $14\ mm \times 40\ mm$ die. When properly clamped, this textured region lies directly over the columnated region of the floor, and interfaces directly with the tops of the columns. The ceiling layer is $16 mm$ longer than the floor, thus providing an overhanging region for out-of-plane heat absorption from a ceramic heater.

Theory of Operation and Measurement

Fig. 2 shows the mechanics of operation of the open-loop micro-evaporator. Liquid water is pumped (via a servo-driven syringe pump) to a reservoir on the backside of the device floor, from where it reaches the top evaporation surface (device ceiling) thorough the hollow columns. Upon contacting the hydrophilic micro-textured ceiling, the liquid spreads out over its surface, and is vaporized by the heat flowing in laterally from the ceramic heater. This newly-formed vapor is ejected from the vapor chamber to ambient by the vapor channels.

The *apparent lateral thermal conductivity* of the evaporation surface can be used to measure the rate of thin-film evaporation in the vapor chamber. In Fig. 3, we illustrate, using an analytical heat transfer model, how liquid evaporation in the vapor chamber affects the temperature distribution of the ceiling, along the length of the device. In the absence of liquid evaporation in the vapor chamber, the temperature varies linearly along the length of the ceiling. This is an expected result from Fourier's law of 1-d conduction.

Modeling the evaporative heat loss using a convection coefficient h, numerical simulations (Fig. 3) show that the temperature gradient dT/dx above the vapor chamber decreases as h is increased. Let's define the apparent lateral thermal conductivity k_a of the ceiling

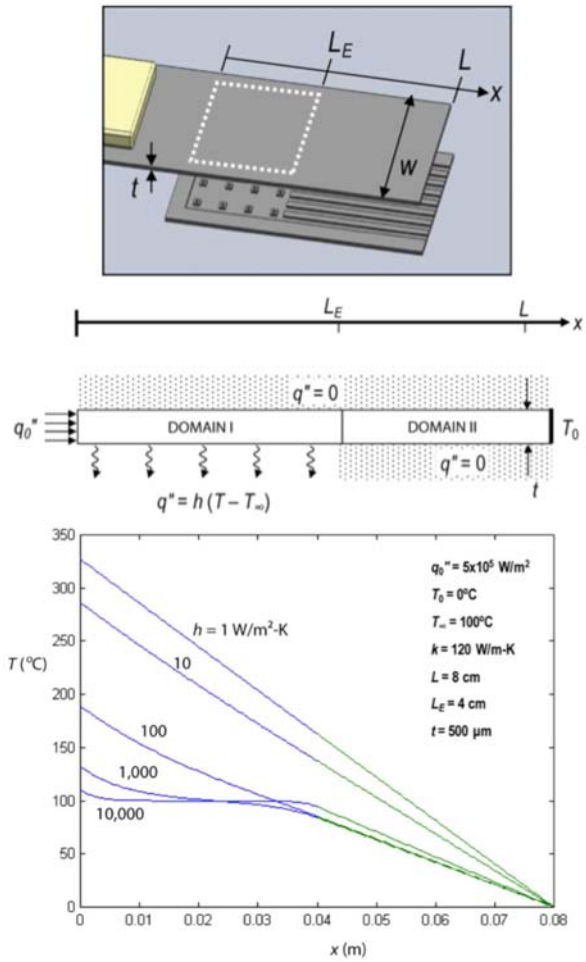

Fig. 3: A model showing the affect of liquid evaporation on the surface temperature distribution of the ceiling, along the length of the device.

above the vapor chamber as follows

$$k_a = \frac{Q}{A_c \left| dT/dx \right|_{x=L_E/2}} \tag{1}$$

where Q is the rate of heat flow in the ceiling along the length of the device, A_c is the area of cross-section of the ceiling, dT/dx is the temperature gradient along the direction of heat flow, and L_E is the length of the vapor chamber. In the absence of lateral evaporative heat losses, k_a will be equal to the solid thermal conductivity of silicon. As the amount of evaporation increases, the apparent thermal conductivity also increases—k_a, therefore, correlates to the amount of thin-film evaporation in the vapor chamber.

Experimental Setup

Fig. 4 shows the experimental setup used to study thin-film evaporation in the micro-evaporator. An infrared camera, placed above the device top surface, was used to track device surface temperatures in real time. Liquid was supplied to the device at a fixed flow rate, via an automatic syringe pump. The power to the ceramic heater was set to a fixed value using an external voltage source. After the fluid flow rate had stabilized,

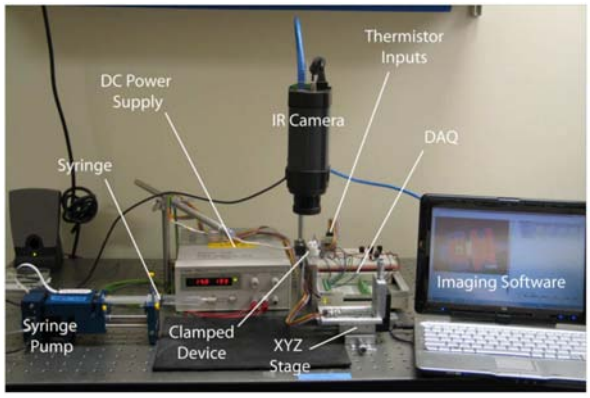

(a)

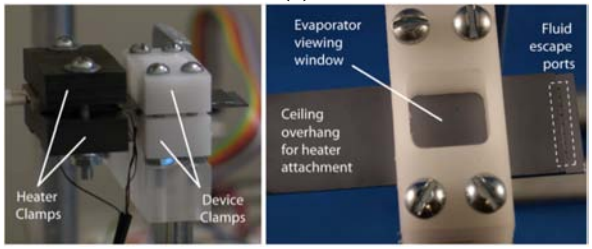

(b)

Fig. 4: The experimental setup: (a) Infrared temperature measurement system (b) Ceramic heater and micro-evaporator assembly.

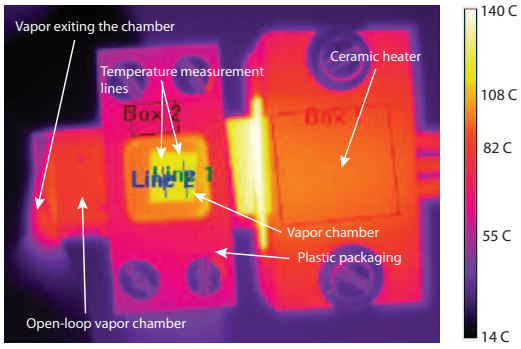

Fig. 5: Infrared image of the top of the micro-evaporator assembly during the evaporation experiments.

the heater was switched on to initiate evaporation in the vapor chamber.

RESULTS AND DISCUSSION

Fig. 5 shows an infrared image of the top of the micro-evaporator assembly during the evaporation experiments. We can see that the portion of the device ceiling near the ceramic heater is the hottest and the temperature drops as we go left towards the vapor exit. For the purpose of calculating the apparent thermal conductivity using Eq. 1, the temperature gradient is measured across the two lines drawn on the vapor chamber. To calculate the rate of heat flow Q across the device, the convective heat losses from the heater clamps are subtracted from the power dissipated by the ceramic heater. Natural convection correlations, which depend only on surface temperatures of the heater clamps, are used to

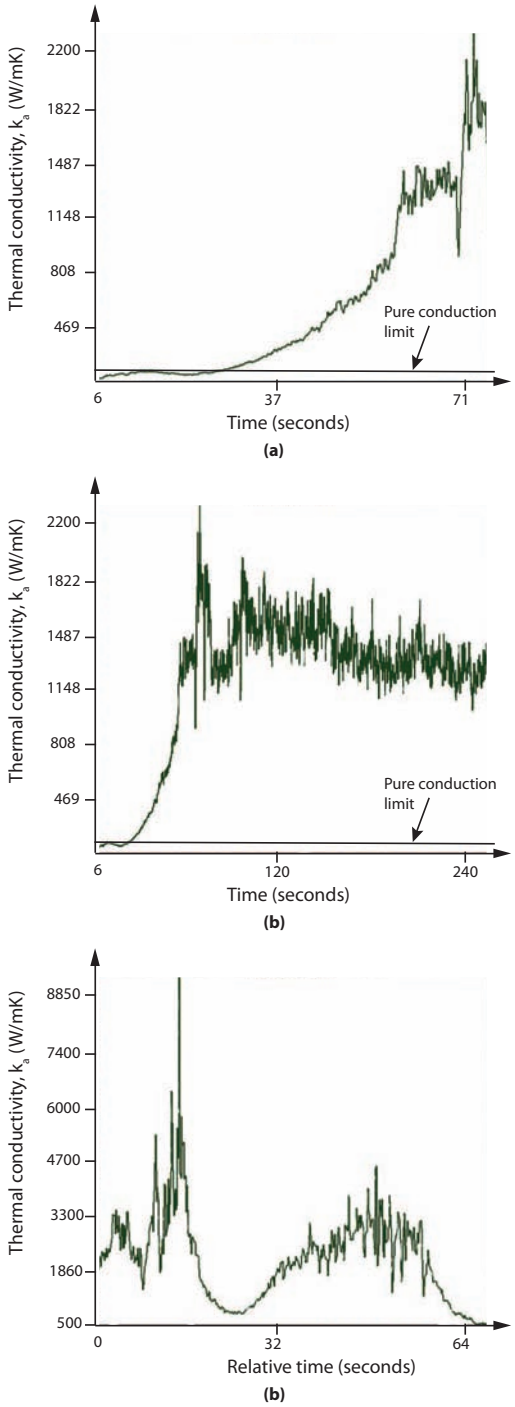

Fig. 6: Experimental results demonstrating the change in apparent thermal conductivity of the vapor chamber due to evaporation: (a) Onset of boiling as the ceramic heater is turned on; (b) Steady state evaporation that follows; (c) A close-up view of the fluctuations in k_a encountered during steady state evaporation at later times.

calculate these convective losses.

The process of thin-film evaporation in the micro-evaporator is demonstrated in Figs. 6(a)-(c) by plotting the apparent thermal conductivity (k_a) of the ceiling above the vapor chamber vs. time. Cold water is provided to the vapor chamber at a flow rate of $4148 \mu L/hr$, and the power supply to the heater is fixed at $4.9\ W$. The trend of the apparent thermal conductivity, after the

heater is switched on, is shown in Fig. 6(a). For the initial 25 seconds the conductivity hovers around a value of $100\ W/mK$, which is close to the thermal conductivity of pure silicon at $100\ ^oC$. During this time, there is no evaporation in the vapor chamber; A finite amount of time is required to heat the incoming liquid to the required saturation temperature for evaporation.

As the process of evaporation sets in, k_a starts to increase gradually (Fig. 6(a)), and eventually reaches an oscillatory steady state (Fig. 6(b)) where $1000\ W/mK < k_a < 2000\ W/mK$. The oscillations become more pronounced as time increases (Fig. 6(c)), with k_a varying between $500 W/mK$ and $9500 W/mK$. Looking at Fig. 6(c), we note that there are low frequency and high frequency components to this oscillatory behavior.

The low frequency oscillations in the value of k_a may be attributed to changes in the overall flow mechanics inside the micro-evaporator. It could be that there is a partial dry-out in the fluid reservoir supplying liquid to the columns, which suppresses evaporation until the time that it has been replenished completely by the liquid inflow from the syringe pump. The high frequency oscillations indicate that the evaporation process in the micro-evaporator is inherently unsteady. This could result from the fact that the liquid inflow into the vapor chamber, which is driven by an external syringe pump, does not necessarily match the rate of evaporation in the chamber. The surplus liquid supply to the evaporation surface interferes with the process of evaporation, thus making it unsteady. This is confirmed by the fact that under normal circumstances a liquid-vapor mixture, and not pure vapor, exits from the vapor exit channels.

CONCLUSIONS

An open-loop micro-evaporator has been designed and fabricated to study the process of phase-change in a columnated wicking structure. A novel *in-plane apparent thermal conductivity* concept has been successfully implemented to measure and characterize thin-film evaporation in the device. Unsteady thin-film evaporation was observed in the vapor chamber, a result attributed to the inherent inconsistency between the rate of liquid supply and rate of evaporation in the open-loop configuration. However, thin-film evaporation was successfully demonstrated in a columnated wicking structure with apparent thermal conductivities as high as $9500\ W/mK$. These results will enable the implementation of a coherent porous silicon based micro-columnated wicking structure.

ACKNOWLEDGMENTS

Defense Advanced Research Projects Agency, Microsystems Technology Office (MTO), Program: Thermal Ground Plane (TGP), Issued by DARPA/CMO under Contract No: HR0011-10-C-0100

REFERENCES

[1] Krishnan S, Garimella S V, Chrysler G M, Mahajan R V 2007 Towards a thermal Moore's law *IEEE Transactions on Advanced Packaging* **30** 462–474

[2] Pastukhov V, Maidanik Y, Vershinin C, Korukov M 2003 Miniature loop heat pipes for electronics cooling *Applied Thermal Engineering* **23** 1125–1135

[3] Singh R, Akbarzadeh A, Mochizuki M 2010 Thermal Potential of Flat Evaporator Miniature Loop Heat Pipes for Notebook Cooling *IEEE Transactions on Components and Packaging Technologies* **33** 32–45

[4] Kirshberg J, Liepmann D, Yerkes K L 1999 Micro-cooler for chip-level temperature control *Aerospace Power Systems Conference* SAE International, Mesa, Arizona SAE Technical Paper Series

[5] Liepmann D 2001 Design and fabrication of a micro-CPL for chip-level cooling *American Society of Mechanical Engineers, Heat Transfer Division, (Publication) HTD* New York, NY, United states vol. 369 51 – 54

[6] Dhillon N S, Pisano A P, Hogue C, Hopcroft M A 2008 MLHP: A high heat flux localized cooling technology for electronic substrates *ASME Conference Proceedings* **2008** 621–630

[7] Dhillon N S, Hogue C, Hopcroft M A, Pisano A P 2010 Geometric control of the fluid-transport meniscus in a passive phase-change microfluidic electronics cooling device *Proceedings of Power MEMS* Leuven, Belgium 15–18

[8] Dhillon N S, Hogue C, Chan M W, Cheng J C, Pisano A P 2011 Integrating coherent porous silicon as a wicking structure in the mems based fabrication of a vertically wicking micro-columnated loop heat pipe *Proceedings of ASME International Mechanical Engineering Congress and Exposition* Denver, CO, United States

[9] Dhillon N S, Cheng J C, Pisano A P 2011 Minimizing the wick thickness in a planar microscale loop heat pipe using efficient thermodynamic design *Proceedings of ASME International Mechanical Engineering Congress and Exposition* Denver, CO, United States

[10] Dhillon N S, Cheng J C, Pisano A P 2011 Heat transfer due to microscale thin film evaporation from the steady state meniscus in a coherent porous silicon based micro-columnated wicking structure *Proceedings of ASME International Mechanical Engineering Congress and Exposition* Denver, CO, United States